Systematic Study of Joint Influence of Angular Resolution and Noise in Cardiac Diffusion Tensor Imaging

Yunlong He[1], Lihui Wang[2,*], Feng Yang[3], Yong Xia[4], Patrick Clarysse[1], and Yuemin Zhu[1,*]

[1] Univ Lyon, INSA Lyon, Université Claude Bernard Lyon 1, CNRS, Inserm, CREATIS UMR 5220, U1294, F-69621, LYON, France (e-mail: Yunlong.He@creatis.insa-lyon.fr; patrick.clarysse@creatis.insa-lyon.fr; Yue-Min.Zhu@creatis.insa-lyon.fr).

[2] Key Laboratory of Intelligent Medical Image Analysis and Precise Diagnosis of Guizhou Province, School of Computer Science and Technology, Guizhou University, Guiyang, China (e-mail: wlh1984@gmail.com).

[3] National Library of Medicine, National Institute of Health, 8600 Rockvill Pike, Bethesda, MD 20894, USA (Feng.yang2@nih.gov).

[4] School of Computer Science, NPU, Xian, China.

Abstract. Diffusion tensor imaging (DTI) is a promising imaging technique to non-invasively study diffusion properties and fiber structures of myocardial tissues. Previous studies have investigated the influence of noise or angular resolution independently on the estimation of diffusion tensors in DTI. However, the joint influence of these two factors in DTI remains unclear. In this paper, we propose to systematically study the joint influence of angular resolutions and noise levels on the estimation of diffusion tensors and tensor-derived fractional anisotropy (FA) and mean diffusivity (MD). The results showed that, as expected, given a certain noise level and sufficient acquisition time, the accuracy of diffusion tensor, FA and MD all increase as the angular resolution. Moreover, when the angular resolution reached a certain value, further increasing the number of angular resolutions has little effect on the estimation of diffusion tensor, FA and MD. Also, both the mean and variance of FA or MD decrease as the angular resolution increases. For an imposed acquisition time, increasing the angular resolution reduces SNR of DW images. When fixing SNR, higher angular resolution can be obtained at the expense of longer acquisition time. These findings suggest the necessity of an optimized trade-off when designing DTI protocols.

Keywords: Diffusion tensor magnetic resonance imaging, angular resolution, fractional anisotropy, mean diffusivity.

* Corresponding author: Lihui Wang and Yuemin Zhu

1 Introduction

Diffusion tensor imaging (DTI) refers to a magnetic resonance imaging (dMRI) technique that measures diffusion of water molecules within biological tissues using diffusion-weighted pulse sequences. DTI makes it possible to explore diffusion properties and fiber structures of tissues non-invasively compared to conventional imaging modalities [1]. In cardiac imaging, for example, DTI has been increasingly used to investigate myocardial microstructure changes related to many cardiac disorders such as hypertrophic cardiomyopathy [2], myocardial infarction [3], etc.

In DTI, water diffusion in tissues is described by diffusion tensors estimated from a set of diffusion-weighted (DW) images associated with noncollinear diffusion gradient directions. The number of gradient directions define the angular resolution. Specifically, it is possible to estimate the diffusion tensor D, a 3×3 symmetric positive definite matrix, according to the Stejskal-Tanner equation [4]: $S_i = S_0 \exp\left(-bg_i^{\mathrm{T}} D g_i\right)$, for $i = 1, 2, \cdots n (n \geq 6)$, where n is the number of diffusion gradient directions, S_i is the DW signal intensity acquired in the i-th gradient direction g_i, and b is the diffusion weighting factor [5]. At a given voxel, the water diffusion properties are quantified by calculating the eigenvalues of the diffusion tensor and tensor-derived measures [6] such as fractional anisotropy (FA) and mean diffusivity (MD).

Accurate estimation of diffusion tensors is important for characterizing water diffusion and thus assessing the myocardial fiber structure. In practice, however, the estimation accuracy of diffusion tensors is influenced by several factors, e.g., image quality, estimation algorithm, tissue complexity, etc. Two factors, noise and angular resolution, have attracted much attention. The noise sources in DW images refer to random signals arising from the hardware (e.g., gradient-coil noise [7], field inhomogeneity [8], etc.) and inherent motions of the subject (e.g., heartbeat and respiration). These noises give rise to perturbed DW signals, and thus produce errors in the calculated diffusion tensor as well as its derived measures. The angular resolution in DTI determined by the number of diffusion gradient directions is used in acquiring DW images. It also influences the estimation of diffusion tensors.

The influence of noise or angular resolution in DTI have been independently investigated by researchers. For example, Pierpaoli et al. [9] show that the MD derived from diffusion tensors decreases as the noise level increases. Anderson in [10] demonstrated that higher noise levels increase the maximum eigenvalue of tensors, and thus result in a larger FA value. For the angular resolution, Papadakis et al. [11] compared various DTI angular sampling schemes, and show that the minimum number of gradient directions for accurate estimation of FA is around $18-21$. Jones [12] found that at least 20 gradient directions are required for robust estimation of FA, and at least 30 directions are required for robust estimation of tensor orientation and MD. Despite these useful findings, it remains unclear how the angular resolution and noise jointly affect the diffusion tensor estimation in DTI.

In this paper, we systematically studied the joint influence of angular resolution and noise in cardiac DTI. Specifically, a set of DW images with different diffusion gradient directions are simulated from a simulated diffusion tensor field. Besides, real datasets of four human hearts are acquired with a large number of diffusion gradient directions. Then, different levels of Rician noise are added to both the simulated and real DW images to produce datasets with different signal-to-noise ratio (SNR). Different angular resolutions of data are achieved by varying the number of considered diffusion gradient directions for each SNR. Finally, the quality of diffusion tensors and tensor-derived FA, MD for different angular resolutions and different noise levels is quantitatively assessed. In addition, the relationship between angular resolution and SNR for a fixed acquisition time is also studied.

The current study has two main contributions. First, this is, to our knowledge, the first work to systematically investigate the joint influence of different angular resolutions and different levels of noise in cardiac DTI. Second, we quantitatively defined the minimum angular resolution required to obtain near-optimal diffusion tensors, FA and MD at a certain noise level, and also investigated the maximum angular resolution for keeping certain SNRs when imposing acquisition time.

2 Materials and methods

2.1 Simulated datasets

Simulated DW data were generated to analyze the influence of angular resolution and noise level on the estimation accuracy of diffusion tensors. The simulation strategy is similar to the method proposed in [13]. Specifically, a $20 \times 20 \times 20$ diffusion tensor field containing 9 homogeneous tensor regions with discontinuities of different amplitudes was created to represent 9 different structures of a human heart. Each z-slice of the tensor field is defined by

$$\begin{pmatrix} R_0 & R_1 & R_0 & R_2 \\ R_0 & R_3 & R_0 & R_4 \\ R_0 & R_5 & R_0 & R_6 \\ R_0 & R_7 & R_0 & R_8 \end{pmatrix} \tag{1}$$

where R_i represents a 5×5 homogeneous region containing 25 of the same diffusion tensors. Here we set these tensors by using the same coefficients as in [13], namely the eigenvalues of each tensor were $(2, 1, 1) \times 10^{-3}$ mm^2/s. The b-value was $700 s/mm^2$, which is the same value that is used in the real cardiac datasets. The FA and MD values for the simulated noisy DW images associated with 12 directions were FA $= 0.33 \pm 0.06$ and MD $= 1.3 \pm 0.11 \times 10^{-3}$ mm^2/s, which are typical for the left ventricular (LV) myocardium of *ex vivo* human hearts (according to the statistical results in [14]).

The simulated DW images were computed from simulated diffusion tensor field using Stejskal-Tanner equation with associated diffusion gradient directions.

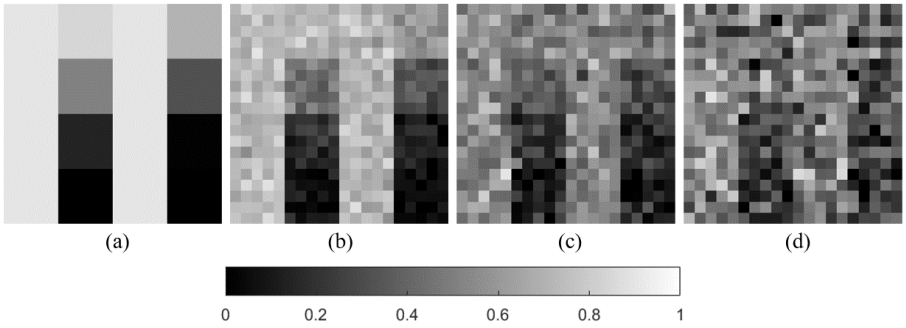

Fig. 1. An example of simulated DW images with: (a) no noise (ground-truth), noise levels with standard deviation (b) $\sigma = 0.02$ ($SNR = 23dB$), (c) $\sigma = 0.05$ ($SNR = 15dB$), and (d) $\sigma = 0.1$ ($SNR = 15dB$). The encoding gradient direction related to the DW image g_i is (0.894, 0 , 0.447).

In order to analyze the effects of noise, different levels of Rician noise [15] were added to the ideal DW images with different standard deviation values. The noise levels of the simulated DW images were measured via SNR (as shown in Fig. 1). Different angular resolutions of DW images were achieved by sampling different number of associated diffusion gradient directions. The sampling method for diffusion gradient directions is detailed in Section 2.3. In this paper, the number of excitations used for signal averaging for each direction was set only when acquisition time is fixed; otherwise, the number was set to 1.

2.2 Real datasets

DTI of *ex vivo* human hearts including two infants and two adults were performed. The infants datasets were acquired in clinical conditions with a Siemens 3T MRI Magnetom Verio. The imaging parameters are the following: $TE = 74ms$, $TR = 7900ms$, FOV $= 144 \times 144mm^2$, slice thickness=$1.4mm$, in-plane resolution = $2mm$, slice spacing = $1.4mm$, slice duration = $123.2ms$, number of slices = 35, slice size: 104×104 pixels, diffusion sensitivity b = $700s/mm^2$, and number of gradient directions = 192, 64 or 12. In each direction, MRI scans were acquired 6 to 10 times for noise reduction. The adult datasets were acquired using Siemens 3T MRI Magnetom Prisma with following parameters: $TE = 71ms$, $TR = 9600ms$, FOV $= 177 \times 177mm^2$, slice thickness=$1.5mm$, slice spacing = $1.5mm$, slice duration = $123.1ms$, number of slices = 70, slice size: 122×122 pixels, diffusion sensitivity b = $700s/mm^2$, and number of gradient directions = 192. In each direction, MRI scans were performed 3 times for noise reduction. An example of real DW images from an infant and an adult is given in Fig. 2.

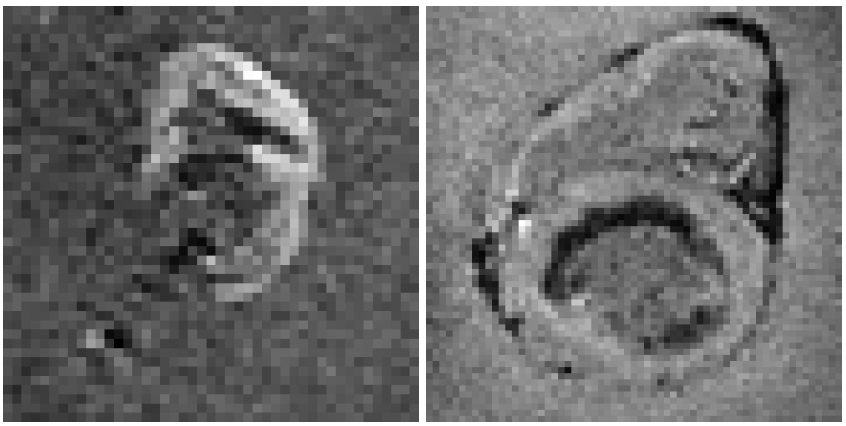

(a) (b)

Fig. 2. An example of DW images from real datasets. (a)An DW image of infant. (b) An DW image of adult.

2.3 Gradient direction sampling

We considered two commonly used angular sampling schemes to generate spherically uniform distributed gradient directions for different angular resolutions of simulated datasets: Spherical Tessellation (ST) [16] and Electrostatic Energy Minimization (EEM) [17]. The ST employs spherical polyhedrons to generate specified numbers of directions geometrically uniformly distributed on a sphere. The EEM is capable of generating an arbitrary number of uniformly distributed directions by minimizing the electrostatic energy based on Coulomb's law. In order to systematically analyze the effects of various angular resolutions, we used EEM to generate different angular resolutions with uniformly-spaced numbers of diffusion gradient directions and one resolution with 6 directions (minimum number of gradient directions required for tensor estimation). For the real datasets, the popular spherical code sampling method [18] was used to obtain different angular resolutions from the real 192 directions. The directions for each subset are uniformly distributed on a sphere.

2.4 Evaluation

In the case of the simulated data, the SNR (dB) is defined by

$$SNR = 20 \cdot \log_{10} \left(\frac{V_n}{\frac{1}{N_v} \|V_n - V_f\|_2} \right) \tag{2}$$

where V_n denotes a discrete volume corrupted by Rician noise and V_f its noise-free representation. $\|\cdot\|$ is the standard Euclidean norm, and N_v is the number

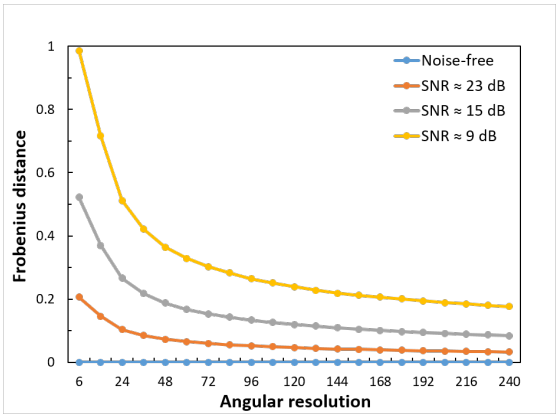

Fig. 3. Differences (Frobenius distance (10^{-3} mm^2/s)) between estimated and ground-truth tensor fields as a function of angular resolution and level of noise.

of voxels. In the case of real cardiac data, the SNR (dB) is defined by

$$SNR = 20 \cdot \log_{10}\left(\frac{\mu_{rm}}{\sigma_{rm}}\right) \tag{3}$$

where μ_{rm} and σ_{rm} are the mean and standard deviation (SD) of the voxel intensity values over the region of the myocardium.

We also evaluated the simulated and real data with different angular resolutions and different levels of noise by estimating diffusion tensors using standard least-squares estimation. The FA and MD were then derived from the diffusion tensors. For the simulated data, the mean Frobenius distance, root mean square errors (RMSE) of FA and MD (In the following sections, we call them FA or MD errors.) between ground-truth (the simulated tensor field) and the estimated diffusion tensors were computed. For the real data, the mean and standard deviation of FA and MD were computed.

3 Results

3.1 Results on simulated data

In Fig. 3, Frobenius distance curves are illustrated for different angular resolutions and different levels of noise. Here the used numbers of diffusion gradient directions were $N_d = \{6, 12, 24, 36, 48, \cdots, 240\}$. From this figure, we can clearly see that for each SNR, Frobenius distance decreases as the angular resolution increases, and that for each angular resolution, the distance decreases as the SNR increases. The vales of Frobenius distances for the maximum angular resolution (240) are smaller than 0.2 even for smaller SNR. Besides, the values of Frobenius distance for the dataset without noise (blue line) are always less

than $= 1.2 \times 10^{-15}$ mm^2/s, which means that varying the angular resolution of noise-free dataset has no impact on the estimated diffusion tensors.

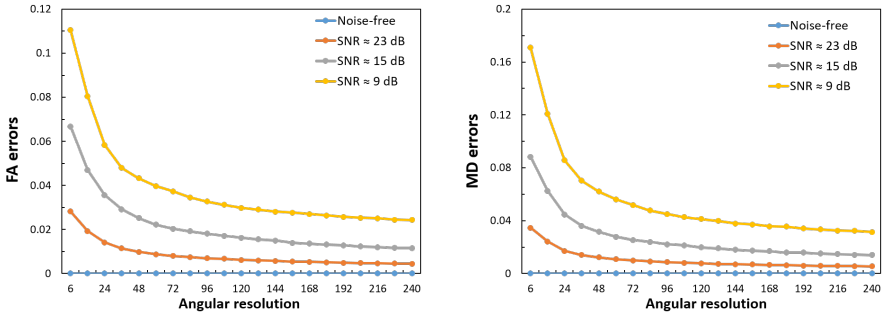

(a) (b)

Fig. 4. Errors on tensor-derived measures for different angular resolution and level of noise. (a) FA errors. (b) MD errors. The unit of MD is 10^{-3} mm^2/s

Fig. 4 shows the curves of FA and MD errors as a function of the angular resolution and noise. The values of FA and MD were computed from the diffusion tensors (corresponding to the results in Fig. 3). From this figure, it can be observed that for all SNRs, the errors of FA or MD decrease as the angular resolution increases. Moreover, for each SNR, there is a tendency for both FA and MD errors to stabilize when the number of diffusion gradients (i.e. angular resolution) reached a certain number. This tendency can also be found in Fig. 3. To describe it clearly, we defined this number as the minimum angular resolution required for which the Frobenius distance, FA or MD errors come within 1% of their range (subtract the minimum value from the maximum value). For example, with this rule, the near-optimal diffusion tensors (the range of Frobenius distances smaller than 0.02) for SNR = 23 dB, 15 dB and 9 dB were achieved with 48, 120 and 156 diffusion gradient directions, respectively. The near-optimal FAs (the range of FA errors smaller than 0.006) for SNR = 23 dB, 15 dB and 9 dB were achieved with 48, 120 and 132 diffusion gradient directions, respectively, while for the near-optimal MDs (the range of MD errors smaller than 0.007), these numbers were 48, 108 and 124, respectively.

Fig. 5 gives the SNR curves as a function of the angular resolution for three acquisition times. To facilitate comparison, we assumed that the scan time for each simulated DW image was approximately 1s, and that the total acquisition time T is defined by the number N_d of diffusion gradient directions multiplied by the number N_e of excitations for each direction (used for signal averages): $T = N_d \times N_e$. Here $N_d = \{6, 12, 18, 24, 30, \cdots, 120\}$ was sampled for achieving different angular resolutions. N_e was set such that for a given angular resolution, we kept roughly the same acquisition time, e.g. $N_e = \{20, 10, 7, 5, 4, \cdots, 1\}$ was

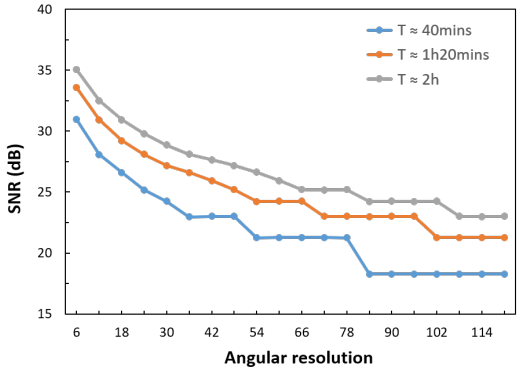

Fig. 5. SNR as a function of angular resolution for three fixed acquisition times. The values of SNR were computed using Eq. (2).

chosen for a acquisition time of approximately 40 minutes. From this figure, we can see that for each acquisition time, the SNR value decreases as the angular resolution increases. Moreover, longer acquisition time allows the use of higher angular resolution while keeping a certain value of SNR. For example, when SNR $\geq$ 25 dB, the maximum available angular resolutions were 25, 48, and 78 for T $\approx$ 40mins, 1h20min, and 2h, respectively.

3.2 Results on real data

Fig. 6 shows how the mean and standard deviation (SD) of FA and MD vary with the angular resolution and noise on real cardiac data. To evaluate the effect of noise, three additional datasets (SNR= 17 dB, 11 dB and 4 dB) were generated by adding different levels of Rician noise to the original DW images. The SNR was computed using Eq. (2), where V_n and V_f are the discrete volume corrupted with Rician noise and without noise, respectively. It can be seen that for all the noisy datasets with different levels of noise, the mean FA and MD value decreases as the angular resolution increases. Besides, the results also show that the MD value decreases as the noise level increases. This is consistent with the results in Pierpaoli et al's study [9]. In Table 1, the mean and SD of FA and MD were estimated for the four real datasets. For higher noise level (e.g., SNR=4), the difference between original and noisy datasets decreases significantly as the angular resolution increases. In addition, when the number of gradient directions are greater than 48, increasing the angular resolution has smaller effects on FA and MD, as also observed on simulated data.

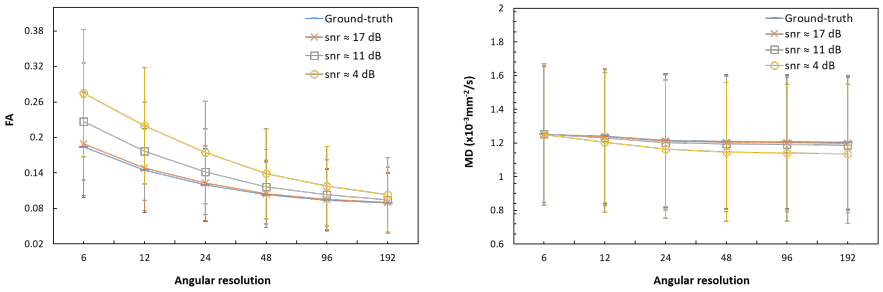

(a) (b)

Fig. 6. Mean±SD of (a) FA and (b) MD values for different angular resolutions and different levels of noise on a real dataset of an infant heart.

Table 1. Mean±SD of FA and MD on four real datasets of *ex vivo* human hearts with different angular resolutions. The unit of MD is 10^{-3} mm^2/s.

	Subject	Number of diffusion gradient directions (i.e., angular resolution)					
		6	**12**	**24**	**48**	**96**	**192**
FA	Infant # 1	0.18 ± 0.08	0.14 ± 0.07	0.12 ± 0.06	0.10 ± 0.06	0.09 ± 0.05	0.09 ± 0.05
	Infant # 2	0.16 ± 0.06	0.12 ± 0.04	0.11 ± 0.04	0.10 ± 0.04	0.10 ± 0.04	0.09 ± 0.04
	Adult # 1	0.22 ± 0.11	0.19 ± 0.11	0.17 ± 0.10	0.16 ± 0.10	0.15 ± 0.10	0.15 ± 0.10
	Adult # 2	0.17 ± 0.08	0.14 ± 0.07	0.13 ± 0.07	0.12 ± 0.06	0.12 ± 0.06	0.11 ± 0.05
MD	Infant # 1	1.31 ± 0.45	1.30 ± 0.45	1.27 ± 0.45	1.27 ± 0.45	1.27 ± 0.45	1.26 ± 0.45
	Infant # 2	1.42 ± 0.33	1.43 ± 0.33	1.42 ± 0.32	1.41 ± 0.32	1.41 ± 0.32	1.41 ± 0.32
	Adult # 1	0.91 ± 0.32	0.87 ± 0.33	0.86 ± 0.34	0.85 ± 0.34	0.84 ± 0.34	0.84 ± 0.34
	Adult # 2	0.90 ± 0.21	0.88 ± 0.22	0.88 ± 0.22	0.87 ± 0.22	0.87 ± 0.22	0.87 ± 0.22

Fig. 7 illustrates the variation of SNR as a function of the angular resolution on a real cardiac dataset (an infant heart) when the acquisition time is fixed to approximately 1h40min. Different angular resolutions were achieved by sampling $N_d = \{32, 38, 44, 50, \cdots, 140\}$ from the original 192 diffusion gradient directions. $N_e = \{6, 5, 4, 3, \cdots, 1\}$ so that we kept a roughly equivalent acquisition time. The step shape occurs in Fig. 7 because for some continuous N_d, a same N_e was set for them in order to make sure that their total acquisition time were closer to 1h40min. For example, for N_d from 62 to 92, the N_e was set to 2; but for $N_d \geq 98$, N_e was set to 1. It can be seen from Fig. 7 that for a fixed acquisition time, SNR decreases as angular resolution increases. Besides, the maximum angular resolution for SNR $\geq$ 12 dB is 62.

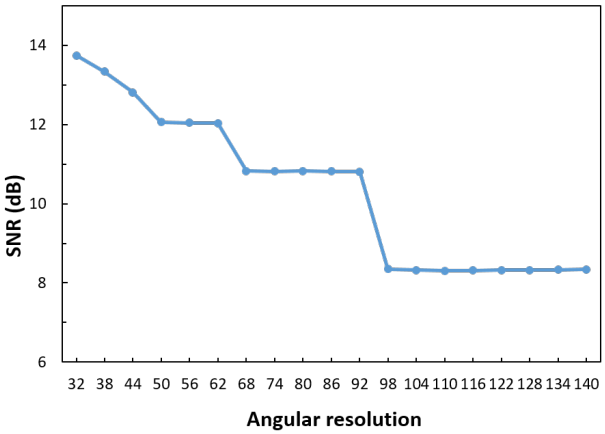

Fig. 7. SNR as a function of the angular resolution for fixed acquisition time on a real cardiac dataset. The values of SNR were computed using Eq. (3).

4 Conclusions and Discussions

This paper investigated the joint influence of angular resolutions and noise levels in cardiac DTI. The results on both synthetic and actual DW images showed that, as expected, given sufficient acquisition time and a certain noise level, the accuracy of diffusion tensors, FA and MD measurements increase as angular resolutions increase. Besides, continuing to increase the angular resolution beyond a certain value has little effect on the accuracy of diffusion tensor, FA and MD. For higher SNR (23 dB), the near-optimal diffusion tensor, FA and MD were obtained with 48 gradient directions. With lower SNR, the near-optimal diffusion tensor, FA and MD were obtained with, for example, 120 directions if SNR = 15 dB and with 156 directions if SNR = 9 dB. In addition, the results on real data show that both the mean and variance of FA or MD decrease as the angular resolution increases. When acquisition time is imposed, increasing angular resolution often comes at the cost of a reduced number of excitations used for signal averaging, thus reducing the SNR of DW images. Longer acquisition times allow the use of higher angular resolution while keeping a certain level of SNR. These findings suggest the necessity of an optimized trade-off when designing DTI protocols. In the future, we would like to conduct a similar study on *in vivo* DTI of the human heart.

Acknowledgements

This work was partly supported by the Program PHC-Cai Yuanpei 2018 (N° 41400TC), the LabEx PRIMES (Physics, Radiobiology, Imaging and Simulation), and the CNRS International Research Project METISLAB.

References

1. David S Tuch, Timothy G Reese, Mette R Wiegell, and Van J Wedeen. Diffusion mri of complex neural architecture. *Neuron*, 40(5):885–895, 2003.
2. Choukri Mekkaoui, Shuning Huang, Guangping Dai, Timothy G Reese, Jeremy Ruskin, Udo Hoffmann, Marcel P Jackowski, and David E Sosnovik. Myocardial infarct delineation in vivo using diffusion tensor mri and the tractographic propagation angle. *Journal of Cardiovascular Magnetic Resonance*, 15(1):1–3, 2013.
3. Ming-Ting Wu, Wen-Yih Tseng, Mao-Yuan Su, Chun-Peng Liu, Kuan-Rau Chiou, Van J Wedeen, Timothy G Reese, and Chien-Fang Yang. Diffusion tensor magnetic resonance imaging mapping the fiber architecture remodeling in human myocardium after infarction: correlation with viability and wall motion. *Circulation*, 114(10):1036–1045, 2006.
4. Edward O Stejskal and John E Tanner. Spin diffusion measurements: spin echoes in the presence of a time-dependent field gradient. *The journal of chemical physics*, 42(1):288–292, 1965.
5. DIVIM Le Bihan. Ivim method measures diffusion and perfusion. 1990.
6. Warren D Taylor, Edward Hsu, K Ranga Rama Krishnan, and James R MacFall. Diffusion tensor imaging: background, potential, and utility in psychiatric research. *Biological psychiatry*, 55(3):201–207, 2004.
7. Robert Hurwitz, Samuel R Lane, RA Bell, and MN Brant-Zawadzki. Acoustic analysis of gradient-coil noise in mr imaging. *Radiology*, 173(2):545–548, 1989.
8. Uro Vovk, Franjo Pernus, and Botjan Likar. A review of methods for correction of intensity inhomogeneity in mri. *IEEE transactions on medical imaging*, 26(3):405–421, 2007.
9. Carlo Pierpaoli and Peter J Basser. Toward a quantitative assessment of diffusion anisotropy. *Magnetic resonance in Medicine*, 36(6):893–906, 1996.
10. Adam W Anderson. Theoretical analysis of the effects of noise on diffusion tensor imaging. *Magnetic Resonance in Medicine: An Official Journal of the International Society for Magnetic Resonance in Medicine*, 46(6):1174–1188, 2001.
11. Nikolaos G Papadakis, Chris D Murrills, Laurance D Hall, Christopher L-H Huang, and T Adrian Carpenter. Minimal gradient encoding for robust estimation of diffusion anisotropy. *Magnetic resonance imaging*, 18(6):671–679, 2000.
12. Derek K Jones. The effect of gradient sampling schemes on measures derived from diffusion tensor mri: a monte carlo study. *Magnetic Resonance in Medicine: An Official Journal of the International Society for Magnetic Resonance in Medicine*, 51(4):807–815, 2004.
13. Carole Frindel, Marc Robini, Pierre Croisille, and Yue-Min Zhu. Comparison of regularization methods for human cardiac diffusion tensor mri. *Medical image analysis*, 13(3):405–418, 2009.
14. Yan-Li Zhang, Wan-Yu Liu, Isabelle E Magnin, and Yue-Min Zhu. Feature-preserving smoothing of diffusion weighted images using nonstationarity adaptive filtering. *IEEE Transactions on Biomedical Engineering*, 60(6):1693–1701, 2013.
15. Hákon Gudbjartsson and Samuel Patz. The rician distribution of noisy mri data. *Magnetic resonance in medicine*, 34(6):910–914, 1995.
16. NA Teanby. An icosahedron-based method for even binning of globally distributed remote sensing data. *Computers & Geosciences*, 32(9):1442–1450, 2006.
17. Derek K Jones, Mark A Horsfield, and Andrew Simmons. Optimal strategies for measuring diffusion in anisotropic systems by magnetic resonance imaging. *Magnetic Resonance in Medicine: An Official Journal of the International Society for Magnetic Resonance in Medicine*, 42(3):515–525, 1999.

18. Jian Cheng, Dinggang Shen, Pew-Thian Yap, and Peter J Basser. Single-and multiple-shell uniform sampling schemes for diffusion mri using spherical codes. *IEEE transactions on medical imaging*, 37(1):185–199, 2017.